Estuarine, Coastal and Shelf Science 199 (2017) 141–151

Contents lists available at ScienceDirect

Estuarine, Coastal and Shelf Science

journal homepage: www.elsevier.com/locate/ecss

An analysis of the relationship between drought events and mangrove changes along the northern coasts of the Pe rsian Gulf and Oman Sea

Davood Mafi-Gholami [a, *], Beytollah Mahmoudi [b], Eric K. Zenner [c]

[a] Department of Forest Sciences, Faculty of Natural Resources and Earth Sciences, Shaherkord University, Rahbar BLVD., Shaherkord, Iran
[b] Department of Forest Sciences, Faculty of Natural Resources and Earth Sciences, Shaherkord University, Shaherkord, Iran
[c] Department of Ecosystem Science and Management, The Pennsylvania State University, Forest Resources Building, University Park, PA 16802, USA

ARTICLE INFO

Article history:
Received 29 May 2017
Received in revised form
29 September 2017
Accepted 10 October 2017
Available online 12 October 2017

Keywords:
Mangroves
Droughts
Area and canopy cover changes
Northern coasts of the Persian Gulf and Oman Sea
Change-point year

ABSTRACT

Relating the changes of mangrove forests to spatially explicit reductions in rainfall amounts and increases in drought occurrences is a prerequisite for improving the effectiveness and success of mangrove forest conservation programs. To this end, we investigated the relationship between drought events (quantified using the Standardized Precipitation Index [SPI]) and changes in area and canopy cover of mangrove forests on the northern coast of the Persian Gulf and the Oman Sea using satellite imagery and long-term annual rainfall data over a period of 30 years (1986–2016). Statistical analyses revealed 1998 as the year marking the most significant change-point in the mean annual rainfall values in the catchments and mangroves, after which average SPI values consistently remained at lower levels. In the period of 1998–2016, decreases in the mean annual rainfall and increases in the severity of droughts differed spatially and were greater in the catchments and mangroves on the coasts of the Oman Sea than the coasts of the Persian Gulf. These spatially explicit results were closely mirrored by the mangrove response, with differential in reductions in mangrove areas and canopy cover that corresponded closely with the spatial distribution of drought intensities in the different parts of the coasts, with correlation coefficients ≥0.89 for the different coastal regions.

1. Introduction

For thousands of years, mangrove forests have played a major role in the economy and sustainable livelihoods of human societies through their unique locations at the interface of terrestrial and aquatic ecosystems (Hamilton et al., 1989; Kaplowitz, 2001). Despite their importance for meeting human needs, degradation and loss of these unique coastal habitats around the world have intensified over the past three decades, so that now more than 50% of the world's mangrove forests have already been destroyed and the trend appears to continue (Alongi, 2002). Among the various factors that have influenced this negative trend, climate change features prominently. Projected consequences of climate change, such as changes in rainfall patterns, increased average temperatures, increased concentration of carbon dioxide, sea level rise, increased storm activities, and changes in ocean circulation patterns already seem to have a significant impact on the growth and development of mangroves all over the world (Urrego et al., 2013; Alongi, 2015; Galeano et al., 2017). Because of a close relationship between mangrove habitat conditions and rainfall, any changes in rainfall patterns and surface water in watersheds will have a significant impact on the growth and spatial distribution of mangroves (Field, 1995; Ellison, 2000). Changes in structure and function of mangroves arise from simultaneous occurrences and synergies among multiple stressors and disturbances (Gilman et al., 2008; Lewis et al., 2011), yet the relationship between mangroves and drought appears to be of fundamental importance (Sakho et al., 2011; Asbridge et al., 2016). Specifically, reduced rainfall and increased drought occurrence can lead to increased evaporation and salinity that can cause a reduction in net primary production, growth and survival, changes in competitive advantages among mangrove species, ultimately leading to further adverse structural changes (reductions of area and canopy), loss of biodiversity, and increased vulnerability of mangroves to other human and natural stresses (Lovelock and Ellison, 2007; Djebou et al., 2015; Brandt et al., 2017).

The premise for this work is that linking changes in drought

* Corresponding author.
E-mail addresses: d.mafigholami@nres.sku.ac.ir (D. Mafi-Gholami), b.mahmoudi@ut.ac.ir (B. Mahmoudi), eric.zenner@psu.edu (E.K. Zenner).

https://doi.org/10.1016/j.ecss.2017.10.008
0272-7714/

occurrence to the location and extent of changes in mangroves may improve the success of conservation and restoration programs that are an integral part of integrated coastal zone management that seeks to identify existential threats and ensure a balance between the economic utilization and cultural values of mangroves (Alongi, 2015). To this end, investigating severity, probability and temporal and spatial variations of droughts is one of the most promising tools for assessing the risk and vulnerability of natural and human environments following climate changes in different regions (Bottero et al., 2017; Young et al., 2017). Various indicators such as the Palmer Drought Severity Index (PDSI) (Palmer, 1965), Standardized Precipitation Index (SPI) (McKee et al., 1993) and Palmer Hydrological Drought Index (PHDI) (Karl and Knight, 1985) have been used for assessing the effects of drought events on natural and human systems. The easy-to-use Standardized Precipitation Index (SPI) has been widely employed to determine the occurrence of drought episodes and enables investigations of water deficiencies at different spatial and temporal scales (Łabędzki, 2017; Khadr, 2017; Kamali et al., 2017). To monitor temporal and spatial changes in natural ecosystems from a variety of environmental factors including droughts across large regions, satellite imagery is increasingly being used (Nascimento et al., 2013; Srivastava et al., 2015; Bamba et al., 2015; Duke et al., 2017). The advantages of satellite images are their synoptic coverage of large areas, the availability of low-cost or free satellite data, the availability of historical satellite data including the repeated coverage of some areas with remotely sensed data (Giri, 2016; Aitkenhead, 2017).

Iran's location in the desert belt (25–40° north latitude) means that average annual rainfall amounts are about one third of the global mean (UNEP, 1997; Rafi Sharif Abad et al., 2016) and rainfall deficiencies and drought occurrences are frequent and severe (Madani et al., 2016). Severe and very severe droughts in recent years have caused significant reductions in the volume of fresh water resources in the Middle East, and especially in Iran (NASA, 2013). Severe to extreme droughts occur more frequently in the southern part of Iran (Gohari et al., 2017) where subtropical high pressure systems prevent the penetration of any pluvial system and, combined with a rise of moist air in the Persian Gulf and the Oman Sea, make rainfall occurrences nearly impossible (Zarei et al., 2016). Since the year 2000, mean annual rainfall and surface water inflow to northern coastal areas of the Persian Gulf and the Oman Sea have been reduced by 43% and 67%, respectively. Here, mangroves that are part of the global network Man & Biosphere and one of the most important mangrove habitats in the Middle East, cover an area of approximately 192 square kilometers (FAO, 2007).

Despite their importance, mangrove ecosystems of Iran are threatened by human utilization for fuel harvest, livestock grazing or aquaculture farming, unmanaged tourism, new industrial development (i.e., the construction of ports, marine transportation), mining, and exposure to pollutants such as industrial and municipal wastewater and oil (Danehkar, 1998; Mehrabian et al., 2009; Zahed et al., 2010). Busy shipping lanes in the Strait of Hormuz receive annual oil discharges of more than 1.5 million tons, which is in addition to large amounts of oil that entered the waters of the region during the Gulf War in 1990 and caused significant damage to mangroves (Majnounian and Danehkar, 1998; Danehkar, 2001; Ebrahimi and Riahi Bakhtiari, 2010) that may take over 20 years to recover (Burns et al., 1993) and prompted the International Maritime Organization (IMO) to designate the region as a special marine region (PGSC, 2017). Further, populations of introduced non-native black rats that thrive with increasing canopy density, diameter, and height of mangroves, and availability of seeds and lush vegetation (Ghadirian et al., 2011; Harper et al., 2015) and decline as canopy cover of the lush mangrove vegetation decreases (Previtali et al., 2009; Russell and Ruffino, 2012; Harper et al., 2015), destroy seeds, trunks, and branches of mangrove trees and put further stress on the ecosystem (King, 2005; Ghadirian et al., 2008, 2011).

Although long-term drought occurrence and significant reductions in rainfall on the southern coasts of Iran are among the most important factors increasing the vulnerability of mangroves (Mafi-Gholami et al., 2015a,b), the effects of drought occurrence on mangroves of Iran have not been quantified yet. In this study, our general aim was to quantify the intensities and trends of droughts and relate those to changes in the structure of mangroves to contribute to timely and effective actions for the protection and restoration of mangroves of Iran. Specifically, we used satellite imagery and long-term rainfall data (1986–2016) for the northern coast of Persian Gulf and the Oman Sea and computed the Standardized Precipitation Index (SPI) to identify the most important change-point year in annual rainfall that indicates a long-term trend in drought occurrence over the 30-year period. Then, we related the SPI and drought occurrences to spatially explicit changes in the area and canopy cover of different mangrove forests and adjacent catchments over the entire 30-year period and separately for the interval before and after the change-point year.

2. Materials and methods

2.1. Study area

The study area consists of mangrove forests composed of two mangrove species Harra (*Avicennia marina*) and Chandal (*Rhizophora mucronata*) located in the Hormozgan province. Mangrove forests of the Hormozgan province occupy the greatest remaining area of this forest type in the country and in the entire of Persian Gulf region, including the waters of ROPME[1] region. The study area comprises 10025.55 ha, is located on the northern coasts of the Persian Gulf and the Oman Sea, and is distributed among seven towns in the area (i.e., Jask, Sirik, Minab, Bandar Abbas, Khamir, Qeshm and Bandar Lengeh). Natural mangrove forests on the coastal areas of Hormozgan range between 25° 34′ 13″ N in Gabrig (Jask town) to 27° 10′ 54″ in Koulaghan (Bandar Abbas town) and 58° 34′ 07″ E in Himan (Jask town) to 55° 22′ 06″ E in Bandar Lenge town (Fig. 2). In these natural sites, mangroves occur in unmixed, irregular and uneven-aged *Avicennia* associations and, in the Syric habitat, mixed *Rhizophora-Avicennia* associations (Majnounian and Danehkar, 1998). At 25–28° northern latitudes, the region has a warm and humid climate, with a high annual mean relative humidity of more than 65 percent (Danehkar, 1998) and long-term mean annual rainfall of about 146 mm and a mean annual temperature of about 27.2 °C. The highest amount of rainfall occurs in January and February; July is the warmest month with a mean temperature of 34.5 °C and January is the coldest month with a mean temperature of 18.1 °C. Recorded absolute maximum and minimum temperatures are 7.5 °C and 48 °C, respectively.

Mangroves on the northern coast of the Persian Gulf and the Oman Sea are classified according to geographical location, habitat structure and geomorphology of the coast and are found in four areas: Khamir, Tiab, Sirik and Jask (Danehkar, 2001). The mangroves of Khamir, Tiab and Jask have been exposed to the least amount of direct impacts by human intervention (such as harvesting twigs), including no afforestation. In contrast, the Sirik habitat, which is located on the west coast of the Persian Gulf, experienced extensive afforestation of about 500 ha with the two species of *Avicenna marina* and *Rhizophora mucronata* in 2010. We therefore restricted our investigation of the relationship between

[1] Regional Organization for Protection Marine Environment (ROPME).

drought occurrence and mangrove changes to the areas of Khamir, Tiab and Jask and excluded the Sirik area from this study. Finally, to facilitate a more detailed investigation of mangrove changes, we divided the mangrove habitats into 8 sites according to the areas covered by each satellite image (Fig. 1).

2.2. Analyzing temporal change of meteorological drought

2.2.1. Standardized precipitation index (SPI)

In general, SPI values of different temporal scales represent different drought impacts on water resources. SPI values that cover short time scales (1–3 months) are indicative of changes in soil moisture that have the potential to greatly affect agriculture. SPI values that cover longer time scales (6 months to one year and more) represent long-term changes in the amounts of precipitation, surface- and underground waters, and water resources in an entire region, with important implications for ecosystem functioning and water resources management in human settlements (Wu et al., 2001). Survival and ability of mangroves to cope with high salinity of water is dependent on the amount of rainfall and surface freshwater entering a region from upstream catchments (Field, 1995; Ellison, 2000). Because responses of mangroves to changes in the amounts of rainfall and volumes of freshwater entering mangrove forests have a three-year delay (Davenport and Nicholson, 1993), we decided to use a 12-month average SPI in this study to assess changes of drought occurrence and determine the change-point in rainfall pattern. The relationship between drought and mangroves areas and canopy cover was carried out for a moving window of three-year intervals. For this purpose, we obtained monthly precipitation data from 16 meteorological stations in the catchments and coastal areas from the Iran Meteorological Organization (IRMO) that covered a 30-year period (1986–2016). To avoid confounding our results with the effect of phenological changes of mangroves over the annual season, only satellite images and SPI values for the month of September were used. The SPI time series were computed following the method described by McKee et al. (1993).

2.2.2. Trend detection

Trend analysis is an essential tool for quantifying the frequency and severity of droughts and for analyzing the relationship between drought occurrence and the occurrence of temporal and spatial changes in ecosystems. There are several statistical methods for detecting trends in data series, but each method has different strengths and weaknesses (Zhang et al., 2008). The Mann-Kendall (MK) test (Kendall, 1975; Mann, 1945) has been recommended by

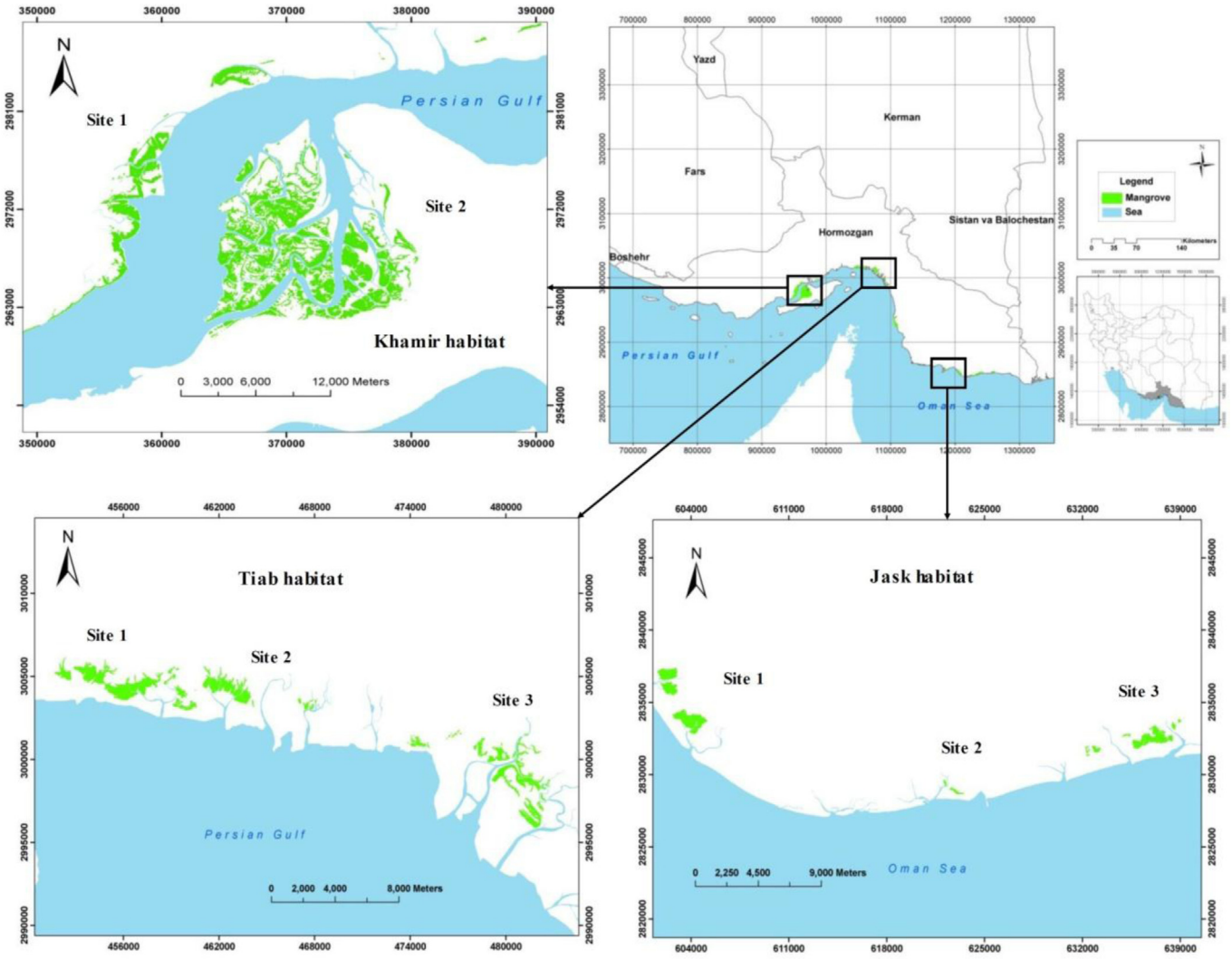

Fig. 1. Geographic location of mangrove habitats on the northern coasts of the Persian Gulf and the Oman Sea.

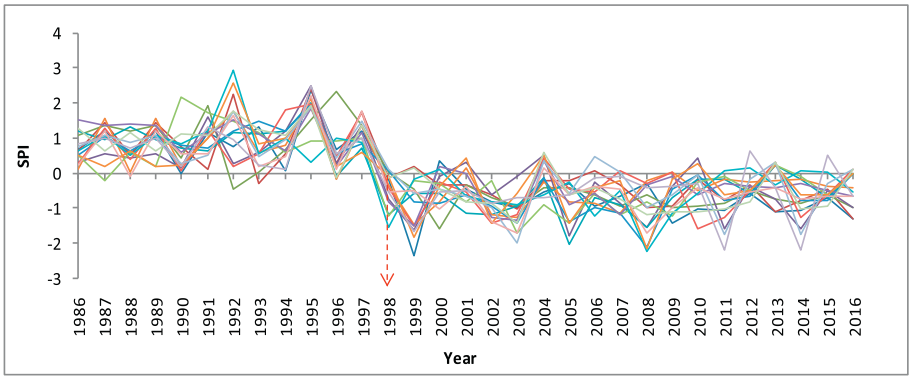

Fig. 2. Changes in drought intensity in the 30-year study period (1986–2016) based on one-year SPI values for September in 16 meteorological stations in the catchments and coastal areas. SPI values above 2 indicate extreme wetness, between 2 and 1 severe to moderate wetness, between 1 and -1 normal conditions, between −1 and −1 moderate to severe droughts, and below −2 extreme droughts.

the World Meteorological Organization (Mitchell et al., 1966). The MK test is one of the most widely used tests for detecting trends in time series of climate variables (Zhang et al., 2012) and was employed in the MAKESENSE 1.0 environment in this study to detect a trend in SPI values.

2.3. Change-point detection in rainfall values

In addition to quantifying a potential trend in drought over time, identifying the change-point or breakpoint in a trend allows a more accurate interpretation of the consequences of drought occurrence and changes in rainfall patterns on ecosystems (Chu et al., 2012). In general, a change-point is defined as the point in time when the frequency distribution of a variable significantly changes direction for a time (Lubes et al., 1998). Among several break tests such as the Pettitt (1979), Buishand (Buishard, 1984), Lee and Heghinian (1977) and Hubert (Hubert et al., 1989) tests that enable detection of changes in a data series, the Pettitt-Mann-Whitney test has been most commonly used for determining the change-point in rainfall and discharge time series data (Kiely, 1999; Nazemosadat et al., 2006; Eslami-Andargoli et al., 2009). This test is a version of the non-parametric Mann-Whitney two-sample test (Pettitt, 1979) that considers the time series as consisting of two samples, i.e., the period before and after a change. The objective of the test is to determine the probability that a given point is a change-point in time series of different lengths (e.g., annual, 6-month, seasonal or monthly) (Maftei et al., 2012). In this study, we calculated the probability for a change-point in a time series using the Pettitt–Mann–Whitney-Test ($\alpha = 0.05$) to identify the year in which the most significant change in annual rainfall amounts occurred and used the cumulative sum method (CUSUM) in the Change Point Analyzer (CPA) software to identify the most significant change-point. The CUSUM method is a simple and tangible method that was originally developed for controlling industrial processes (Barratt et al., 2007), can be used in trend data regardless of the nature of data (Chelani, 2011), and has been used in environmental monitoring programs for detecting the change-point in time series of environmental variables (Carslaw et al., 2006; Barratt et al., 2007; Andersen et al., 2009), including climatic variables (Kampata et al., 2008; Li et al., 2008; Eslami-Andargoli et al., 2009; Chowdhury and Beecham, 2010; Chu et al., 2012; Maftei et al., 2012). Finally, after identifying a change-point, the significance of the change at that point was confirmed with a *t*-test by comparing the means of annual rainfall before and after the identified year.

2.4. Mangrove change detection

2.4.1. Data sources

Ninety Landsat satellite images (path/row # 158/042, 159/041 and 160/041) for the month of September were obtained for a 30-year period (1986–2016). Landsat images were used because of the limited availability of satellite images with higher resolution. Since cloud cover reduces the image quality and causes errors in detecting the phenomena of interest in the images, we used only images from the Landsat satellite archive that were free of cloud cover. Further, only images from the month of September when the sea level was at low tide were analyzed to prevent potential bias due to phenological differences arising from the change of seasons. For each year in the 30-year image time series, the mean values of area and canopy cover of mangrove forests were calculated.

2.4.2. Image analysis

Determination of exact boundaries of mangrove forests is an important first step for assessing changes over time and requires that images are geometrically corrected for very high precision. Although Landsat C images are generally characterized by good geometric precision, we recorded a total of 250 ground control points using GPS with good distribution throughout the study area to ensure maximum possible accuracy. For detection of the image, Landsat C images of 2016 with a root mean square error lower than one pixel (in this study, RMS = 0.143) were georeferenced with the IDRISI software. Finally, the corrected images of Landsat C were used for geometric correction of Landsat TM images taken in 1986 and 1998. None of the RMS values of the Landsat TM images in any of the corrections was higher than 0.18. All images were georeferenced to UTMWGS-1984 Site 40N projection and datum.

2.4.3. Image classification

Maximum likelihood estimation is one of the most efficient classification methods for extracting mangroves from satellite images with medium spatial resolution (Wang et al., 2004; Giri et al., 2011; Nguyen et al., 2013). Hence, we used supervised classification with a maximum likelihood algorithm for image classification and extraction of mangrove vegetation. To separate mangroves from surrounding water and coastal land areas and to draw the final borders of the study sites, the NDVI vegetation index, which is one of the best and most widely used indices for quick and easy identification of green vegetation from surrounding areas, was computed (Richard and Poccard, 1998; Seto and Fragkias, 2007; Vo et al., 2013). After preparing the NDVI and using false color composites by bands of green, red and near-infrared, images were

classified using supervised classification. In addition, to maximize the accuracy of the boundaries of mangroves, the off-shore (marine) borders of mangroves were manually digitized using precise visual interpretation on a scale of 1:10,000 and with the help of a team of experts. Finally, we used onscreen digitization, which is one of the best approaches for extracting boundaries of fringe mangroves when using medium resolution satellite imagery (Wang et al., 2003; Ellison and Zouh, 2012; Nguyen et al., 2013).

2.4.4. Post-classification analysis, accuracy assessment and social survey

A post-classification filtering process was applied to remove isolated pixels or noise from the classification outputs. The filtered classified images were used as the final land-use map for each year. For accuracy assessment of the maps derived from the classified images of 2015 and 2016, 210 sampling plots with dimensions of 30 × 30 m (900 square meters) were established throughout the study area and the landward and seaward edges of mangroves. Further, aerial photos, land use maps and Quickbird images of the years 1985, 1992, 1995, 2001, 2004, 2009 and 2012 were used to assess classification accuracy of other mangrove maps. Following recommendations by Eslami-Andargoli et al. (2010) and Nguyen et al. (2013), stratified random sampling was used to assess the classification accuracies of the final maps, which enables the computation of user accuracy, producer accuracy and overall accuracy for maps. Mangrove areas were computed for sub-sites, sites and each habitat area. Finally, the mean annual rates of change in mangrove areas were computed for the period before and after the break-point in the time series of annual precipitation. To aid in interpreting our results of changes over time in the areas of mangroves, we compared our results to the results of previous studies (Mahdavi et al., 2005) and conducted face to face interviews with indigenous people and experts. For this purpose, 25 people aged between 50 and 60 years who resided in the region for more than 30 years were interviewed and their comments used to place our results in context.

2.4.5. Mapping mangrove canopy cover percentage

In general, there is a high correlation between Normalized Difference Vegetation Index (NDVI) and mangrove canopy closure (Jensen et al., 1991). To investigate the changes over time in percent canopy closure of mangroves, we followed the method by Giri et al. (2007) that uses the range of changes in NDVI values as a proxy for the changes in mangrove canopy closure. Following the computation of NDVI values for all images, NDVI values equal to 0.2 ($NDVI_{min}$) and 0.7 ($NDVI_{max}$) were assumed to represent open and closed mangrove forests, respectively. The NDVI range of 0.5 was then used to scale percent canopy closure between 0% and 100%, where 0% corresponds to the $NDVI_{min}$ and 100% corresponds to the $NDVI_{max}$. Finally, annual changes in percent of mangrove canopy closure were computed for the 30-year study period for the habitats of Khamir, Tiab and Jask. Because of variation in atmospheric conditions at the time of capturing the images in different years, the reliability of absolute values of canopy closure was enhanced by visual confirmation of the validity of the canopy closure using results of National Iranian Mangrove Forest document (CENRS, 2010), Quickbird images of 2004, and field surveys conducted in 2015 and 2016.

2.5. Analysis of the relationship between SPI and magrove area and canopy changes

In this final step, Pearson correlation coefficients were used to relate SPI values to the mean area and mean canopy cover of mangroves during the 30-year study period in each of the habitats of Khamir, Tiab and Jask.

3. Results

3.1. Spatial and temporal patterns of SPI

The depiction of one-year SPI values shows the temporal dynamics of below and above normal precipitation distribution throughout the study area (Fig. 2). After a moderate to extreme wet period that lasted until the late 1990s, significantly reduced SPI values were observed in the period between 1998 and 2016 that indicate severe and extreme droughts. Based on the temporal patterns of wet and dry years, the 30-year time series of SPI values can clearly be separated into two time periods: a 12-year period between 1986 and 1998 when almost all years exhibited positive SPI values with moderate to extreme wet years and an 18-year period between 1998 and 2016 when generally negative SPI values between 0 to less than −2 reflect a significant decrease in annual rainfall and a long-term and severe drought period.

Major parts of the study area were characterized by decreasing SPI values, indicating that the drying tendency dominated major parts of the region and that the intensity of droughts increased during the period of 1986–2016 (Fig. 3). Sub-basins and coastal areas of the central and eastern parts (i.e., habitats of Tiab and Jask) had a greater tendency for drought than the western parts (i.e., the Khamir habitat). Eastern catchments and coastal areas (i.e., the Jask habitat) had the highest absolute Z-values ($|Z| \geq 3.80$) and exhibited the greatest and most significant tendency for drought among all study areas.

3.2. Rainfall values analysis

The Pettit-Mann-Whitney method revealed that 1998 was the year with the highest probability of being the main change-point year in the 30-year time series of annual rainfall in all of the 16 synoptic climate stations (Fig. 4). There was a significant change in mean annual rainfall before and after 1998 with a reduction between 44 and 83 percent ($P < 0.01$). This was confirmed by the CUSUM method (Fig. 4) and t-tests that revealed statistically significant differences of mean annual rainfall between the two periods pre- and post-1998 across all weather stations ($p < 0.005$) (Table 1).

3.3. Analysis of mangrove area and canopy closure changes in the periods pre- and post-1998

Overall accuracy, user accuracy and producer accuracy of all classified images consistently exceeded 90%, which indicates a high level of accuracy in the classification and mapping of mangroves. The analysis of the time series of satellite images showed significantly different trends in mean annual rates of change in area and mean canopy cover of mangroves in the different habitats between the periods of pre- and post-1998 (Table 2 and Fig. 5). Before 1998, mean annual rates of change in mangrove areas were positive in all sites in all three habitats (i.e., increasing areas), which changed to consistently negative values in all sites in all three habitats after 1998. The mean annual rates of area changes for the all three habitats combined showed gains of 1.99 ha yr^{-1} pre-1998 and losses of −1.25 ha yr^{-1} post-1998, resulting in a significant difference between the two periods ($p \leq 0.001$). Site 2 in the Khamir habitat exhibited the greatest annual rates of area increase among all habitats and sites in the pre-1998 period (Table 2). Overall, the Khamir habitats showed the greatest change in area between pre-1998 and post-1998 of all habitats. All sites in the Tiab habitat and the Jask habitat exhibited negative rates of change in areas

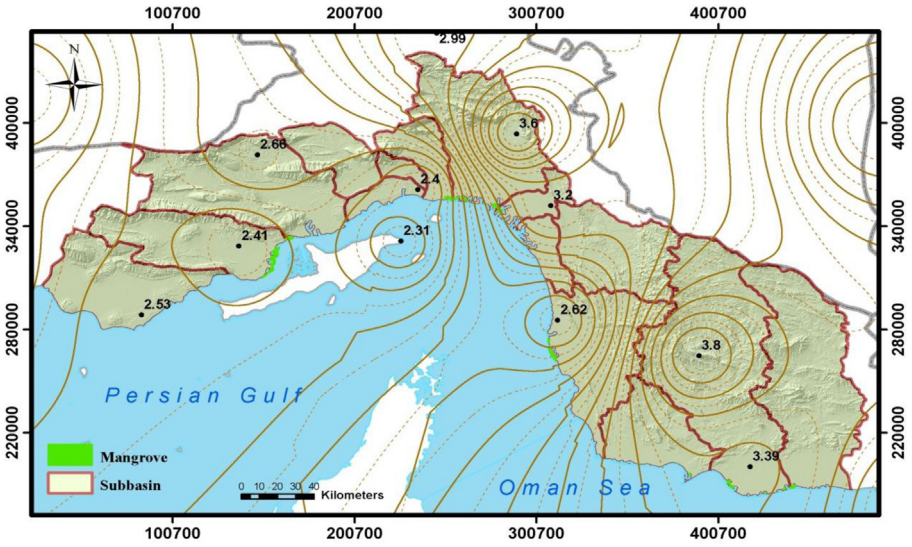

Fig. 3. Spatial distribution pattern of trends of SPI values. The numbers in the figure refer to Z-values. Positive values indicate an increasing trend for drought. Values of $|Z| \geq 1.96$ indicate a statistically significant trend at the >95% confidence level.

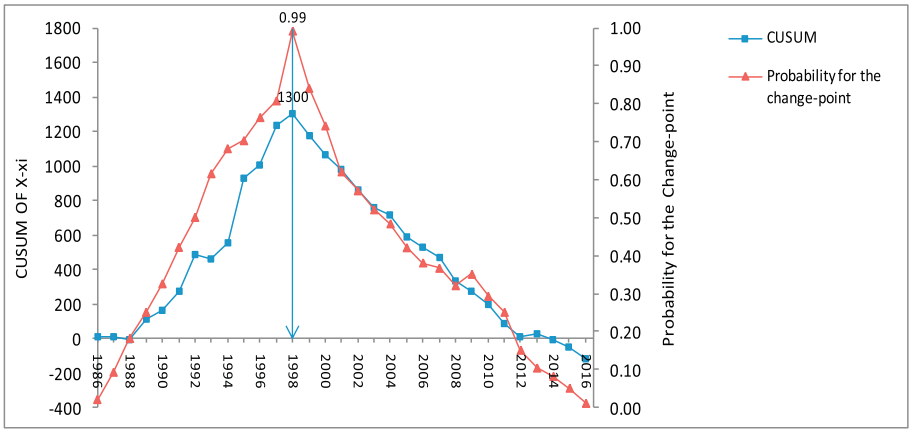

Fig. 4. Result of the Pettitt–Mann–Whitney-Test (probability for the change-point) and the CUSUM for annual rainfall across the study area, which identified 1998 as the change-point year.

Table 1
Changes of mean annual rainfall pre- and post- 1998.

Station	Year (Change point)	Mean annual rainfall Pre-1998 (mm/yr)	Mean annual rainfall Post-1998 (mm/yr)	Reduction in mean annual rainfall (%)	p-value
Bandarabbas	1998	163.94	91.57	44	0.002
Minab	1998	237.71	125.89	47	0.002
Gheshm	1998	205.02	78.40	62	0.003
Jask	1998	188.20	73.37	61	0.001
Chabahar	1998	121.87	20.19	83	0.000
Lengeh	1998	170.82	83.05	51	0.004
Sirik	1998	260.44	100	62	0.000
Abumusa	1998	138.35	63.45	54	0.002
Darab	1998	251.73	130.52	48	0.001
Dayer	1998	344.19	137.54	60	0.005
Hajiabad	1998	325.11	125.31	61	0.004
Kahnuj	1998	256.33	128.31	50	0.002
Kish	1998	199.41	93.52	53	0.006
Lar	1998	249.64	136.15	46	0.002
Lamerd	1998	274.19	158.23	44	0.001
Siri	1998	164.65	74.63	55	0.005

Table 2
Mean annual change in mangrove area and mean canopy cover pre- and post-1998 at all three study habitats.

Study Habitats	Site	Mean annual rate of area change pre-1998 (ha yr^{-1})	Mean annual rate of area change post-1998 (ha yr^{-1})	Mean of canopy closure pre-1998 (%)	Mean of canopy closure post-1998 (%)
Khamir	1	1.47	−0.91	80	73.25
	2	7.65	−0.75	92	85
Tiab	1	2.28	−0.95	91	84.2
	2	3.04	−0.55	89.6	84.3
	3	0.62	−0.63	89	72.9
Jask	1	0.39	−1.57	81	70
	2	0.13	−1.75	79.6	67
	3	0.44	−1.80	72.2	61.2

post-1998, with the greatest overall annual rate of reduction in area (−1.71 ha yr^{-1}) observed in the Jask habitats and the maximum annual rate observed in Site 3 (Table 2).

Similarly, mean mangrove canopy cover decreased in all sites of all three habitats between the post-1998 to the pre-1998 periods (Table 2). Averaged over all three habitats, mean percent canopy covers of 84.3% (pre-1998) and 74.73% (post-1998) differed significantly between the two periods ($p = 0.001$) and decreased by 9.57%. Smallest (5.3%) and greatest (12.6%) reductions were observed in site 2 (Tiab) and site 2 (Jask), respectively. On average, the Tiab habitat exhibited the lowest reduction (5.98%) and the Jask habitat the greatest reduction (11.55%) between pre-1998 and post-1998 (Table 2).

3.4. Analysis of the relationship between SPI and mangrove area and canopy cover changes

Averaged over three-year intervals, mangrove areas and canopy cover were significantly related to SPI values in all three study areas (all p-values ≤ 0.001) and decreased with decreasing SPI values (i.e., reduced annual rainfall and more droughty conditions). The coefficients of determination of each linear regression (R^2) exceeded 0.89 in all three habitats (Table 3).

4. Discussion

The strong climate signal in this study revealed a clear trend of decreasing SPI values and annual amounts in rainfall and, combined with simultaneous reductions in mangrove areas and canopy cover on the northern coast of the Persian Gulf and the Oman Sea, indicate that climate change has already resulted in adverse effects on mangrove forests (Gilman et al., 2008; Eslami-Andargoli et al., 2009; Alongi, 2015). Following the expansion of mangroves in all three studied habitats during a wetter period prior to 1998, their extent and canopy cover declined steadily with the onset of sudden, regular, and significant reductions in annual rainfall and increased severity and duration of droughts. The change-point year in the 30-year time series of annual rainfall (1986–2016) was determined using time series analyses of both SPI and annual rainfall, and did not arbitrarily divide rainfall time series into 10-year periods (Wilton, 2002) nor limit the analysis to annual rainfall data without using long-term drought data (Eslami-Andargoli et al., 2009). This may explain why the change-point year of 1998 coincides well with increased activities of subtropical high pressure systems (Halabian and Shabankari, 2010) that prevent the penetration of pluvial systems inland and can cause severe to extreme droughts on the northern coast of the Persian Gulf and the Oman Sea (Zarei et al., 2016). Since 1998, extensive, severe, and continuous drought occurrences have been reported for all regions of Iran and are likely due to the effectiveness and continuity of the strongest La Niña of the last half century (Barlow et al., 2002; Wilton, 2002). In a similar study conducted in the Morton Bay, the main change-point year in a 32-year time series of rainfall (1972–2004) was the year 1990, and the ensuing drought occurrence between 1990 and 2003 has been attributed to the El Niño phenomenon (Eslami-Andargoli et al., 2009). However, changes in mangrove areas along the coasts of Morton Bay, a region with the same rainfall pattern as in our study area, were more variable (Eslami-Andargoli et al., 2009) and lacked the strong correspondence between mangrove area reductions and increasing drought intensities and changes in rainfall pattern seen in this study.

Overall decreases in mangrove areas of −1.11 ha yr^{-1} are similar to the −1 ha yr^{-1} reported for the 10-year period between 1994 and 2004 by Mahdavi et al. (2005). The decreases were spatially variable across the region, however, and closely followed the spatial rainfall distribution pattern and intensity of droughts, with more intense declines in rainfall, more severe drought occurrences, and greater mangrove losses in the eastern catchments and coastal areas of the Sea of Oman (−1.71 ha yr^{-1} [Jask]) compared to the central and western shores of the Persian Gulf (−0.83 ha yr^{-1} [Khamir] and −0.71 ha yr^{-1} [Tiab]; Fig. 3). A similar pattern with increasing droughts was seen for mangrove canopy cover, which might be an early warning sign of future area loss. While decreasing SPI values, rainfall amounts, surface water flows, and more frequent droughts are the ultimate causes for the reductions in area and canopy cover of mangroves associated with climate change, the proximate causes such as changes in the water salinity, amount of nutrients, and sediment in mangrove beds (Ellison, 2000; Eslami-Andargoli et al., 2009; Lewis et al., 2011; Djebou et al., 2015; Brandt et al., 2017) more directly impact growth, structure and the spatial distribution of mangroves (Snedaker, 1995; Field, 1995; Ellison, 2000) and might help explain some of the differences in the responses among the three habitats in this study and between this and other studies.

The combination of a semi-desert climate, exposure to increased air temperatures, reduced rainfall, long-term droughts, and a reduction in surface runoff and freshwater flow into coastal areas can lead to ~6 times higher evapotranspiration rates than the combined rainfall and river discharge rates (INIOAS, 2017a), which caused large increases in sea water salinity in all studied habitats in excess of tolerance levels of mangrove species (Bahrami Samani et al., 2010; INIOAS, 2017b). This may at least partly explain the retrogression of the landward margins and the loss of area of mangroves in this (Fig. 5) and in other parts of the world (Field, 1995; Ellison, 1993, 2000; Ellison and Farnsworth, 2001; Woodroffe, 1995). Increased salinity, which might even rise further given the documented long-term trends in the variation of temperature and salinity levels of the world's open waters (Bindoff et al., 2007; Talley et al., 2015), has been shown to reduce growth and production, and increase the vulnerability of mangroves to the effects of climate change (Saenger and Snedaker, 1993; Snedaker, 1995; Ball, 2002).

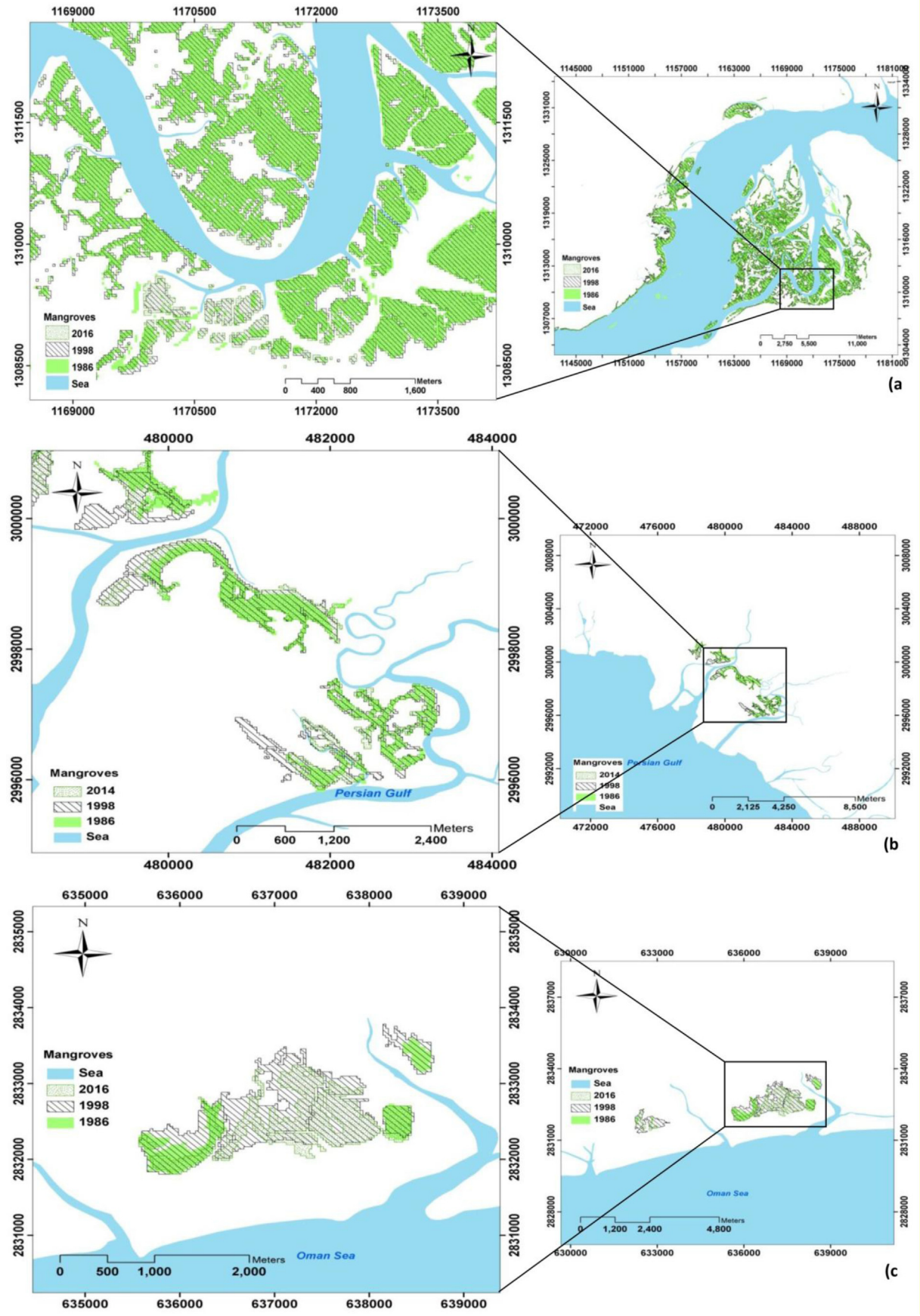

Fig. 5. Changes of areas of mangrove forests in the Khamir (a), Tiab (b), and Jask (c) habitats.

Table 3
Relationships between SPI and mangrove area and canopy cover changes in the Khamir, Tiab and Jask habitats.

Khamir			Jask			Sirik				
Area	Cover	SPI	Area	Cover	SPI	Area	Cover	SPI		
_	–	–	–	–	–	0.90[a]	0.96[a]	1	SPI	Sirik
_	–	–	–	–	–	0.90[a]	1	0.96[a]	Cover	
_	–	–	–	–	–	1	0.90[a]	0.90[a]	Area	
_	–	–	0.91[a]	0.89[a]	1	–	–	–	SPI	Jask
_	–	–	0.88[a]	1	0.89[a]	–	–	–	Cover	
_	–	–	1	0.88[a]	0.91[a]	–	–	–	Area	
0.93[a]	0.94[a]	1	–	–	–	–	–	–	SPI	Khamir
0.85[a]	1	0.94[a]	–	–	–	–	–	–	Cover	
1	0.85[a]	0.93[a]	–	–	–	–	–	–	Area	

[a] Correlation is significant at the 0.01 level (two-tailed).

Sea currents, tidal ranges, and sea level also affect coastal erosion and sedimentation in mangroves (Furukawa et al., 1997). More powerful sea currents along the Oman Sea may explain higher levels of coastal erosion and mangrove loss [Jask] than on the coasts of the Persian Gulf and in the Strait of Hormuz [Khamir and Tiab] (Nohegar and Hosseinzadeh, 2011). Sea level rise induced by climate change also affects ecosystem changes, zonation, and vulnerability of mangroves (Ellison, 2000, 2008; McKee et al., 2007; Gilman et al., 2007; Soares, 2009; Urrego et al., 2013), but its effect on mangroves is relative to concurrent sedimentation rates. Relative to sedimentation rates of 6.2 mm yr^{-1} [Khamir] and 7.3 mm yr^{-1} [Tiab] (Etemadi, 2014), the 4.6 mm yr^{-1} sea level rise predicted by regression models covering the 36-year period between 1980 and 2016 indicate that mangroves are able to keep pace with the relative sea-level rise in the Persian Gulf. In contrast, sedimentation rates of 3.1 mm yr^{-1} [Jask] (Etemadi, 2014) are lower than the rate of sea level rise of 5.5 mm yr^{-1} in the Oman Sea and may explain the greater loss of mangrove area in this habitat in recent years.

In addition to direct and indirect effects of climate change, site-specific characteristics and local environmental factors that include geomorphological characteristics, wetland microtopography, hydrological dynamics of surface and groundwater, upland habitat sediment composition, and human activities that result in different degrees of catchment modification (Ellison, 2000; Eslami-Andargoli et al., 2009; Lewis et al., 2011; Djebou et al., 2015; Brandt et al., 2017) likely affected coastal sedimentation differentially in the three habitats in this study. Geomorphology of the upstream catchment areas and the freshwater delivery by the rivers that drain them can strongly affect sedimentation rates and the expansion and spatial patterns of deltaic mangrove forests (Danehkar, 2001). Whereas the rivers Mehran, Minab, Shoor and Kal [Khamir and Tiab] continue to deposit large amounts of sediments from the easily erodible Makran formation into the shallow beds of the mangroves and enhance the development of coastal plains (Danehkar, 2001; Nohegar and Hosseinzadeh, 2011), the construction of a dam on the River Jagin in 2008 [Jask] has caused a significant decline in the historically large sediment delivery following rainfall events and torrential flows, which might have contributed to a doubling of mean annual rates of areal decline and halving the sedimentation rate in Jask compared to Khamir and Tiab. Dam construction has consistently resulted in a smaller, lower quality mangrove ecosystems due to changed flow paths of rivers and altered volume flows and sedimentary loads to downstream coastal areas (Hashimoto, 2001; Dahdouh Gubas et al., 2005; Ellison and Zouh, 2012). Geological characteristics at the distance between the axial length of the folding and the coastline as well as slope differences of the foreshores can further enhance sedimentation rates on the coastal bed if rivers that enter the coastal plain encounter a decrease in slope [Khamir and Tiab] compared to areas where the slope remains steeper [Jask].

We conclude that this study revealed a strong climate-induced signal that directly affected mangrove ecosystems through reductions in annual rainfall and increases in drought occurrences, but that other causes indirectly related to climate change such as changes of sea water salinity and sea levels as well as human activities such as dam construction and may have exacerbated adverse climatic effects. The analytical method of simultaneously using time series of SPI values and annual rainfall values employed in this study may serve as a basis for investigating the effects of spatial and temporal changes of droughts on other mangrove ecosystems around the world. Specifically, the identification of 1998 as the change-point year at which rainfall patterns shifted in this study may prove useful to climate scientists who may attempt to cross-date related phenomena or to mangrove scientists interested in the speed of mangrove responses to droughts. Based on forecasts that predict reduced rainfall amounts at low latitudes and subtropical areas due to climate change (Solomon et al., 2007), the use of satellite imagery and atmospheric general circulation models is a powerful tool to detect spatially explicit changes in mangrove conditions in subtropical regions and low latitudes in a timely manner.

Acknowledgments

We thank two anonymous reviewers for their constructive comments that have assisted greatly in the revision of the paper. We thank the Iranian National Institute for Oceanography and Atmospheric Science for providing the primary data. We are also grateful to Masumeh Baharlouii for assistance with the image analysis.

References

Aitkenhead, M.J., 2017. Mapping peat in Scotland with remote sensing and site characteristics. Eur. J. Soil Sci. 68 (1), 28–38.
Alongi, D.M., 2002. Present state and future of the world's mangrove forests. Environ. Conserv. 29, 331–349.
Alongi, D.M., 2015. The impact of climate change on mangrove forests. Curr. Clim. Change Rep. 1 (1), 30–39.
Andersen, T., Carstensen, J., Hernandez-Garcia, E., Duarte, C.M., 2009. Ecological thresholds and regime shifts: approaches to identification. Trends Ecol. Evol. 24 (1), 49–57.
Asbridge, E., Lucas, R., Ticehurst, C., Bunting, P., 2016. Mangrove response to environmental change in Australia's Gulf of Carpentaria. Ecol. Evol. 6 (11), 3523–3539.
Bahrami Samani, L., Ebrahimi, M., Ghorbanli, M., 2010. Study of horizontal and vertical distribution of physic & chemical parameters and chlorophyll a in Hormoz Strait. J. Mar. Sci. Technol. 3, 1–17 (In Persian, with English abstract).
Ball, M.C., 2002. Interactive effects of salinity and irradiance on growth:

implications for mangrove forest structure along salinity gradients. Trees 16, 126–139.
Bamba, A., Dieppois, B., Konaré, A., Pellarin, T., Balogun, A., Dessay, N., Kamagaté, B., Savané, I., Diédhiou, A., 2015. Changes in vegetation and rainfall over west Africa during the last three decades (1981-2010). Atmos. Clim. Sci. 5, 367–379.
Barlow, M., Cullen, H., Lyon, B., 2002. Drought in central and southwest Asia: La Nina, the warm pool, and Indian Ocean precipitation. J. Clim. 15 (7), 697–700.
Barratt, B., Atkinson, R., Anderson, H.R., Beevers, S., Kelly, F., Mudway, I., Wilkinson, P., 2007. Investigation into the use of the CUSUM technique in identifying changes in mean air pollution levels following introduction of a traffic management scheme. Atmos. Environ. 41 (8), 1784–1791.
Bindoff, N.L., Willebrand, J., Artale, V., Cazenave, A., Gregory, J., Gulev, S., Hanawa, K., Le Quéré, C., Levitus, S., Nojiri, Y., others, 2007. Observations: oceanic climate change and sea level. In: Solomon, S., Qin, D., Manning, M., Chen, Z., Marquis, M., Averyt, K.B., Tignor, M., Miller, H.L. (Eds.), Climate Change 2007: the Physical Science Basis, Contribution of Working Group I to the Fourth Assessment Report of the Intergovernmental Panel on Climate Change. Cambridge University Press, Cambridge, United Kingdom, and New York, NY, USA, pp. 385–432.
Bottero, A., D'Amato, A.W., Palik, B.J., Bradford, J.B., Fraver, S., Battaglia, M.A., Asherin, L.A., 2017. Density-dependent vulnerability of forest ecosystems to drought. J. Appl. Ecol. Available online: https://doi.org/10.1111/1365-2664.12847.
Brandt, M., Tappan, G., Diouf, A.A., Beye, G., Mbow, C., Fensholt, R., 2017. Woody vegetation die off and regeneration in response to rainfall variability in the west African Sahel. Remote Sens. 9 (1), 39.
Buishard, T., 1984. Tests for detecting a shift in the mean of hydrological time series. J. Hydrol. 58, 51–69.
Burns, K., Garrity, S.D., Levings, S.C., 1993. How many years until mangrove ecosystems recover from catastrophic oil spills?, 26 (5), 239–248.
Carslaw, D.C., Ropkins, K., Bell, M.C., 2006. Change-point detection of gaseous and particulate traffic-related pollutants at a roadside location. Environ. Sci. Technol. 40 (22), 6912–6918.
Consulting Engineers of Nature and Resource Sustainability (CENRS), 2010. National Iranian Mangrove Forest Document, 530 p.
Chelani, A.B., 2011. Change detection using CUSUM and modified CUSUM method in air pollutant concentrations at traffic site in Delhi. Stoch. Environ. Res. Risk Assess. 25 (6), 827–834.
Chowdhury, R.K., Beecham, S., 2010. Australian rainfall trends and their relation to the southern oscillation index. Hydrol. Process. 24 (4), 504–514.
Chu, H.J., Pan, T.Y., Liou, J.J., 2012. Change-point detection of long-duration extreme precipitation and the effect on hydrologic design: a case study of south Taiwan. Stoch. Environ. Res. Risk Assess. 26 (8), 1123–1130.
Dahdouh-Guebas, F., Jayatissa, L.P., Di Nitto, D., Bosire, J.O., LoSeen, D., Koedam, N., 2005. How effective were mangroves as a defense against the recent tsunami? Curr. Biol. 15, 443–447.
Danehkar, A., 1998. Marine sensitive areas of Iran. Environ. Sci. Q. J. 24, 28–38 (In Persian, with English abstract).
Danehkar, A., 2001. Mangroves forests zonation in Gaz and Harra international wetlands. Environ. Sci. Q. J. 34, 43–49 (In Persian, with English abstract).
Davenport, M.L., Nicholson, S.E., 1993. On the relation between rainfall and the normalized difference vegetation index for diverse vegetation types in East Africa. Int. J. Remote Sens. 14 (12), 2369–2389.
Djebou, D.C.S., Singh, V.P., Frauenfeld, O.W., 2015. Vegetation response to precipitation across the aridity gradient of the southwestern United States. J. Arid Environ. 115, 35–43.
Duke, N.C., Kovacs, J.M., Griffiths, A.D., Preece, L., Hill, D.J., Van Oosterzee, P., Burrows, D., 2017. Large-scale dieback of mangroves in Australia's Gulf of Carpentaria: a severe ecosystem response, coincidental with an unusually extreme weather event. Mar. Freshw. Res. 68, 1816–1829.
Ebrahimi, Z., Riahi Bakhtiari, A., 2010. In: Determination of Oil Pollution Based on the Determination of the Concentration of Polycyclic Aromatic Hydrocarbons (PAHs) in Surface Sediments of Mangrove Forests of Bandar Khamir Coasts, the First National Conference on Technology Development in Oil, Gas and Petrochemical Industries. Southern Petroleum Science Institute, Ahwaz, 13p.
Ellison, J., 1993. Mangrove retreat with rising sea level, Bermuda. Estuar. Coast. Shelf Sci. 37, 75–87.
Ellison, J., 2000. How South Pacific mangroves may respond to predicted climate change and sea level rise. In: Gillespie, A., Burns, W. (Eds.), Climate Change in the South Pacific: Impacts and Responses in Australia, New Zealand, and Small Islands States. Kluwer Academic Publishers, Dordrecht, Netherlands (Chapter 15), pp. 289–301.
Ellison, J.C., 2008. Long-term retrospection on mangrove development using sediment cores and pollen analysis: a review. Aquat. Bot. 89 (2), 93–104.
Ellison, A.M., Farnsworth, E.J., 2001. Mangrove communities. Mar. community Ecol. 423–442.
Ellison, J.C., Zouh, I., 2012. Vulnerability to climate change of mangroves: assessment from Cameroon, Central Africa. Biology 1 (3), 617–638.
Eslami-Andargoli, L., Dale, P.E.R., Sipe, N., Chaseling, J., 2009. Mangrove expansion and rainfall patterns in Moreton Bay, Southeast Queensland, Australia. Estuar. Coast. Shelf Sci. 85 (2), 292–298.
Eslami-Andargoli, L., Dale, P.E.R., Sipe, N., Chaseling, J., 2010. Local and landscape effects on spatial patterns of mangrove forest during wetter and drier periods: Moreton Bay, Southeast Queensland, Australia. Estuar. Coast. Shelf Sci. 89 (1), 53–61.
Etemadi, H., 2014. Assessing and Predicting the Effects of Climate Change on Mangrove Forests of Southern Iran. Ph. D. thesis. Tarbiat Modares University, Faculty of Natural Resources, 345 p. (In Persian, with English abstract).
FAO (Food and Agriculture Organization of the United Nations), 2007. The World's Mangroves 1980–2005. FAO Forestry Paper 153. FAO, Rome.
Field, C., 1995. Impacts of expected climate change on mangroves. Hydrobiologia 295, 75–81.
Furukawa, K., Wolanski, E., Mueller, H., 1997. Currents and sediment transport in mangrove forests. Estuar. Coast. Shelf Sci. 44 (3), 301–310.
Galeano, A., Urrego, L.E., Botero, V., Bernal, G., 2017. Mangrove resilience to climate extreme events in a Colombian Caribbean Island. Wetl. Ecol. Manag. Available online: https://doi.org/10.1007/s11273-017-9548-9.
Ghadirian, T., Karami, M., Danehkar, A., Hemami, M.R., 2008. Estimation of nest density and factors influencing the nest selection of black Rattus (Rattus rattus) in mangrove forests of hara Biosphere reserve. Environ. Sci. Technol. 11 (4), 650–657 (In Persian, with English abstract).
Ghadirian, T., Karami, M., Danehkar, A., Hemami, M.R., 2011. Population and density estimate of black rat (Rattus rattus) in mangrove forests in hara Biosphere reserve – Hormozgan province. J. Nat. Environ. Iran. J. Nat. Resour. 64 (2), 145–153 (In Persian, with English abstract).
Gilman, E., Ellison, J., Coleman, R., 2007. Assessment of mangrove response to projected relative sea-level rise and recent historical reconstruction of shoreline position. Environ. Monit. Assess. 124 (1), 105–130.
Gilman, E.L., Ellison, J., Duke, N.C., Field, C., 2008. Threats to mangroves from climate change and adaptation options: a review. Aquat. Bot. 89 (2), 237–250.
Giri, C., 2016. Observation and monitoring of mangrove forests using remote sensing: opportunities and challenges. Remote Sens. 8, 783.
Giri, C., Pengra, B., Zhu, Z., Singh, A., Tieszen, L.L., 2007. Monitoring mangrove forest dynamics of the Sundarbans in Bangladesh and India using multi-temporal satellite data from 1973 to 2000. Estuar. Coast. Shelf Sci. 73 (1), 91–100.
Giri, C., Ochieng, E., Tieszen, L.L., Zhu, Z., Singh, A., Loveland, T., Duke, N., 2011. Status and distribution of mangrove forests of the world using earth observation satellite data. Glob. Ecol. Biogeogr. 20 (1), 154–159.
Gohari, A., Mirchi, A., Madani, K., 2017. System dynamics evaluation of climate change adaptation strategies for water resources management in Central Iran. Water Resour. Manag. 31 (5), 1413–1434.
Halabian, A.H., Shabankari, M., 2010. Synoptic analysis of relationship between subtropical high pressure at 600 hPa level and daily precipitation in Iran. Geogr. Res. 25 (2), 47–82 (In Persian, with English abstract).
Hamilton, L., Dixon, J., Miller, G., 1989. Mangroves: an undervalued resource of the land and the sea. Ocean Yearbk. 8, 254–288.
Harper, G.A., van Dinther, M., Russell, J.C., Bunbury, N., 2015. The response of black rats (Rattus rattus) to evergreen and seasonally arid habitats: informing eradication planning on a tropical island. Biol. Conserv. 185, 66–74.
Hashimoto, T.R., 2001. Environmental Issues and Recent Infrastructure Development in the Mekong Delta: Review, Analysis and Recommendations with Particular Reference to Large-scale Water Control Projects and the Development of Coastal Areas. Working Paper No. 4. Australian Mekong Resource Centre, University of Sydney, 70 p.
Hubert, P., Carbonnel, J.P., Chaouche, A., 1989. Segmentation des séries hydrométéorologiques—application à des séries de précipitations et de débits de l'Afrique de l'ouest. J. Hydrol. 110 (3), 349–367.
Iranian National Institute for Oceanography and Atmospheric Science (INIOAS), 2017a. http://www.inio.ac.ir/Default.aspx?tabid=2029. Last accessed: 22.07.2017.
Iranian National Institute for Oceanography and Atmospheric Science (INIOAS), 2017b. http://www.inio.ac.ir/Default.aspx?tabid=2604. Last accessed: 17.08.2017.
Jensen, J.R., Lin, H., Yang, Y., Ramsey, E., Davis, B.A., Thoemke, C.W., 1991. The measurement of mangrove characteristics in Southwest Florida using SPOT multispectral data. Geocarto Int. 2, 13–21.
Kaplowitz, M., 2001. Assessing mangrove products and services at the local level: the use of focus groups and individual interviews. Landsc. Urban Plann. 56 (1), 53–60.
Kamali, B., Houshmand Kouchi, D., Yang, H., Abbaspour, K.C., 2017. Multilevel drought hazard assessment under climate change scenarios in semi-arid regions-a case study of the Karkheh river basin in Iran. Water 9 (4), 241.
Kampata, J.M., Parida, B.P., Moalafhi, D.B., 2008. Trend analysis of rainfall in the headstreams of the Zambezi river basin in Zambia. Phys. Chem. Earth, Parts A/B/C 33 (8), 621–625.
Karl, T., Knight, R.W., 1985. Atlas of monthly Palmer hydrological drought indices (1931-1983) for the contiguous United States. Natl. Clim. Data Cent.
Kendall, M.G., 1975. Rank Correlation Methods. Griffin, London.
Khadr, M., 2017. Temporal and spatial analysis of meteorological drought characteristics in the upper Blue Nile river region. Hydrol. Res. 48 (1), 265–276.
Kiely, G., 1999. Climate change in Ireland from precipitation and streamflow observations. Adv. Water Resour. 23 (2), 141–151.
King, C.M., 2005. The Handbook of New Zealand Mammals, second ed. Oxford University Press. 610p.
Lee, A.F., Heghinian, S.M., 1977. A shift of the mean level in a sequence of independent normal random variables-a bayesian approach. Technometrics 19 (4), 503–506.
Lewis, M., Pryor, R., Wilking, L., 2011. Fate and effects of anthropogenic chemicals in mangrove ecosystems: a review. Environ. Pollut. 159 (10), 2328–2346.
Li, Z.L., Xu, Z.X., Li, J.Y., Li, Z.J., 2008. Shift trend and step changes for runoff time

series in the Shiyang River basin, northwest China. Hydrol. Process. 22 (23), 4639–4646.
Lovelock, C.E., Ellison, J.C., 2007. Vulnerability of mangroves and tidal wetlands of the Great Barrier Reef to climate change. In: Johnson, J.E., Marshall, P.A. (Eds.), Climate Change and the Great Barrier Reef: a Vulnerability Assessment. Great Barrier Reef Marine Park Authority and Australian Greenhouse Office, Australia, pp. 237–269.
Lubes-Niel, H., Masson, J., Paturel, J., Servat, E., 1998. Variabilité climatique et statistiques. Etude par simulation de la puissance et de la robustesse de quelques tests utilisés pour vérifier l'homogénéité de chroniques. Rev. Sci. l'Eau 11 (3), 383–408.
Madani, K., AghaKouchak, A., Mirchi, A., 2016. Iran's socio-economic drought: challenges of a water-Bankrupt. Natl. Iran. Stud. 49 (6), 997–1016 (In Persian, with English abstract).
Mafi-Gholami, D., Feghhi, J., Danehkar, A., Yarali, N., 2015a. Prioritizing stresses and disturbances affecting mangrove forests using Fuzzy Analytic Hierarchy Process (FAHP). Case study: mangrove forests of Hormozgan Province, Iran. Adv. Environ. Sci. 7 (3), 442–459.
Mafi-Gholami, D., Feghhi, J., Danehkar, A., Yarali, N., 2015b. Classification and prioritization of negative factors affecting on mangrove forests using Delphi method (a case study: mangrove forests of Hormozgan province, Iran). Adv. Biores. 6 (3), 78–92.
Maftei, C., Bărbulescu, A.C., Buta, D.T., 2012. Statistical analysis of precipitation time series in Dobrudja region. MAUSAM 63 (4), 553–564.
Mahdavi, A., Zobeiri, M., Namiranian, M., 2005. Investigation of quaintly and quality changes of mangroves of Gheshm using aerial photographs of 1967 and 1994. J. Nat. Resour. 55 (3), 377–386 (In Persian with English abstract).
Majnounian, H., Danehkar, A., 1998. National parks and marine and coastal protected areas. Case study: Nayband Bay. Environ. Sci. Q. J. 24, 65–74 (In Persian with English abstract).
Mann, H.B., 1945. Nonparametric tests against trend. Econometrica 13, 245–259.
McKee, T.B., Doesken, N.J., Kleist, J., 1993. The relationship of drought frequency and duration to time scales. In: Proceedings of the 8th Conference on Applied Climatology (17(22), 179–183). American Meteorological Society, Boston, MA.
McKee, K.L., Cahoon, D.R., Feller, I.C., 2007. Caribbean mangroves adjust to rising sea-level through biotic controls on change in soil elevation. Glob. Ecol. Biogeogr. 16, 545–556.
Mehrabian, A., Naqinezhad, A., Mahiny, A.S., Mostafavi, H., Liaghati, H., Kouchekzadeh, M., 2009. Vegetation mapping of the mond protected area of Bushehr province (South-west Iran). J. Integr. Plant Biol. 51 (3), 251–260.
Mitchell, J.M., Dzerdzeevskii, B., Flohn, H., Hofmeyr, W.L., Lamb, H.H., Rao, K.N., Wallen, C.C., 1966. Climate Change. WMO Publ. No. 195, Geneva.
Nascimento, W.R., Souza-Filho, P.W.M., Proisy, C., Lucas, R.M., Rosenqvist, A., 2013. Mapping changes in the largest continuous Amazonian mangrove belt using object-based classification of multisensor satellite imagery. Estuar. Coast. Shelf Sci. 117, 83–93.
National Aeronautics and Space Administration(NASA), 2013. Available online: https://www.nasa.gov/mission_pages/Grace/news/grace20130212.html. Last accessed: 20 02 2017.
Nazemosadat, M.J., Samani, N., Barry, D.A., 2006. ENSO forcing on climate change in Iran: precipitation analysis. Iran. J. Sci. Technol. Trans. B Eng. 30 (ECOL-ARTICLE-2007–006), 555–565.
Nguyen, H.H., McAlpine, C., Pullar, D., Johansen, K., Duke, N.C., 2013. The relationship of spatial–temporal changes in fringe mangrove extent and adjacent land-use: case study of Kien Giang coast, Vietnam. Ocean Coast. Manag. 76, 12–22.
Nohegar, A., Hosseinzadeh, M.M., 2011. Sea dynamics and factors affecting sea level fluctuations in the development of the northern Delta of the Strait of Hormuz. J. Geogr. Environ. Plan. 43 (3), 125–142 (In Persian, with English abstract).
Palmer, W.C., 1965. Meteorological Drought, vol. 30. US Department of Commerce, Weather Bureau, Washington, DC, USA.
Pettitt, A.N., 1979. A non-parametric approach to the change-point problem. Appl. Stat. 126–135.
Persian Gulf Studies Center (PGSC), 2017. Available online http://www.persianguIfstudies.com/fa/index.asp?p=pages&id=205.
Previtali, M.A., Lima, M., Meserve, P.L., Kelt, D.A., Gutierrez, J.R., 2009. Population dynamics of two sympatric rodents in a variable environment: rainfall, resource availability, and predation. Ecology 90, 1996–2006.
Rafi Sharif Abad, J., Nohegar, A., Zehtabian, G., Khosravi, H., Gholami, H., 2016. Study of desertification status based on a sub-IMDPA model for a case study in Yazd-Ardakan plain, Iran. Int. J. For. Soil Eros. (IJFSE) 6 (3), 73–81.
Richard, Y., Poccard, I., 1998. A statistical study of NDVI sensitivity to seasonal and interannual rainfall variations in Southern Africa. Int. J. Remote Sens. 19, 2907–2920.
Russell, J.C., Ruffino, L., 2012. The influence of spatio-temporal resource fluctuations on insular rat population dynamics. Proc. R. Soc. Ser. B, Biol. Sci. 279, 767–774.
Saenger, P., Snedaker, S., 1993. Pantropical trends in mangrove aboveground biomass and litterfall. Oecologia 96, 293–299.
Sakho, I., Mesnage, V., Deloffre, J., Lafite, R., Niang, I., Faye, G., 2011. The influence of natural and anthropogenic factors on mangrove dynamics over 60 years: the Somone Estuary, Senegal. Estuar. Coast. Shelf Sci. 94 (1), 93–101.
Seto, K.C., Fragkias, M., 2007. Mangrove conversion and aquaculture development in Vietnam: a remote sensing-based approach for evaluating the Ramsar Convention on Wetlands. Glob. Environ. Change 17 (3), 486–500.
Snedaker, S.C., 1995. Mangroves and climate change in the Florida and Caribbean region: scenarios and hypotheses. In: Asia-Pacific Symposium on Mangrove Ecosystems. Springer, Netherlands, pp. 43–49.
Soares, M.L.G., 2009. A conceptual model for the responses of mangrove forests to sea level rise. J. Coast. Res. 56, 267–271.
Solomon, S., Qin, D., Manning, M., Chen, Z., Marquis, M., Averyt, K., Tignor, M.M.B., Miller, H.L., 2007. Climate Change 2007: the Physical Science Basis. Cambridge University Press, 996 pp.
Srivastava, P.K., Mehta, A., Gupta, M., Singh, S.K., Islam, T., 2015. Assessing impact of climate change on Mundra mangrove forest ecosystem, Gulf of Kutch, western coast of India: a synergistic evaluation using remote sensing. Theor. Appl. Climatol. 120 (3–4), 685–700.
Talley, L.D., Feely, R.A., Sloyan, B.M., Wanninkhof, R., Baringer, M., Bullister, J.L., Gruber, N., 2015. Changes in ocean heat, carbon content, and ventilation: a review of the first decade of GO-SHIP Global Repeat Hydrography.
UNEP, 1997. Word Atlas of Desertification, second ed. John Wiley and Sons, Inc, and Arnold. 182p., New York and London.
Urrego, L.E., Correa-Metrio, A., González, C., Castaño, A.R., Yokoyama, Y., 2013. Contrasting responses of two Caribbean mangroves to sea-level rise in the Guajira Peninsula (Colombian Caribbean). Palaeogeogr. Palaeoclimatol. Palaeoecol. 370, 92–102.
Vo, Q.T., Oppelt, N., Leinenkugel, P., Kuenzer, C., 2013. Remote sensing in mapping mangrove ecosystems—an object-based approach. Remote Sens. 5 (1), 183–201.
Wang, J., Rich, P.M., Price, K.P., 2003. Temporal responses of NDVI to precipitation and temperature in the central Great Plains. USA. Int. J. Remote Sens. 24 (11), 2345–2364.
Wang, Q., Tenhunen, J., Dinh, N.Q., Reichstein, M., Vesala, T., Keronen, P., 2004. Similarities in ground-and satellite-based NDVI time series and their relationship to physiological activity of a Scots pine forest in Finland. Remote Sens. Environ. 93 (1), 225–237.
Wilton, K.M., 2002. Coastal Wetland Habitat Dynamics in Selected New South Wales Estuaries. Ph. D. Thesis. Australian Catholic University, Victoria, Australia. P. 329.
Woodroffe, C.D., 1995. Response of tide dominated mangrove shorelines in Northern Australia to anticipated sea level rise. Earth Surf. Process. Landf. 20 (1), 65–85.
Wu, H., Hayes, M.J., Weiss, A., Hu, Q., 2001. An evaluation of the standardized precipitation index, the China-Z index and the statistical Z-score. Int. J. Climatol. 21 (6), 745–758.
Young, D.J., Stevens, J.T., Earles, J.M., Moore, J., Ellis, A., Jirka, A.L., Latimer, A.M., 2017. Long-term climate and competition explain forest mortality patterns under extreme drought. Ecol. Lett. 20 (1), 78–86.
Zahed, M.A., Rouhani, F., Mohajeri, S., Bateni, F., Mohajeri, L., 2010. An overview of Iranian mangrove ecosystems, northern part of the Persian Gulf and Oman Sea. Acta Ecol. Sin. 30 (4), 240–244.
Zarei, A.R., Moghimi, M.M., Mahmoudi, M.R., 2016. Analysis of changes in spatial pattern of drought using RDI index in south of Iran. Water Resour. Manag. 30 (11), 3723–3743.
Zhang, S., Lu, X.X., Higgitt, D.L., Chen, C.T.A., Han, J., Sun, H., 2008. Recent changes of water discharge and sediment load in the Zhujiang (Pearl River) Basin, China. Glob. Planet. Change 60 (3), 365–380.
Zhang, Q., Li, J., Singh, V.P., Bai, Y., 2012. SPI-based evaluation of drought events in Xinjiang, China. Nat. Hazards 64 (1), 481–492.
Łabędzki, L., 2017. Categorical forecast of precipitation Anomaly using the standardized precipitation index SPI. Water 9 (1), 8.